2017 International Nuclear Atlantic Conference - INAC 2017
Belo Horizonte, MG, Brazil, October 22-27, 2017
ASSOCIAÇÃO BRASILEIRA DE ENERGIA NUCLEAR - ABEN

Agência Brasileira do ISBN
ISBN 978-85-99141-07-6
9 788599 141076

TRANSIENT HEAT TRANSFER ANALYSIS UP TO DRYOUT IN 3D FUEL RODS UNDER UNIDEAL CONDITIONS THROUGH THE DEVELOPMENT OF A COMPUTER CODE

Rodolfo I. Martins[1,a], Renato R. W. Affonso[1], Maria de Lourdes Moreira[1] and Paulo A. B. De Sampaio[1]

[1]Instituto de Engenharia Nuclear (IEN/CNEN)
Cidade Universitária - Ilha do Fundão
Rua Hélio de Almeida 75,
21941-972 Rio de Janeiro, RJ

[a]rodolfoienny@gmail.com

ABSTRACT

In this paper we analyze a conjugated transient heat transfer problem consisting of a nuclear reactor's fuel rod and its intrinsic coolant channel. Our analysis is made possible through a computer code being developed at the Instituto de Engenharia Nuclear (IEN/CNEN). This code is meant to study the temperature behavior in fuel rods which exhibit deviation from their ideal conditions, that is, rods in which the cladding is deformed or the fuel is dislocated. It is also designed to avoid the use of the computationally expensive Navier-Stokes equations. For these reasons, its physical model has as basis a three-dimensional fuel rod coupled to a one-dimensional coolant channel, which are discretized using the finite element method. Intending to study accidental conditions in which the coolant (light water) transcends its saturation temperature, turning into vapor, a homogeneous mixture is used to represent the two-phase flow, and so the coolant channel's energy equation is described using enthalpy. Owing to the fact that temperature and enthalpy are used in the physical model, it became impractical to generate a fully coupled method for solving the pertinent equations. Thus, the conjugated heat transfer problem is solved in a segregated manner through the implementation of an iterative method. Finally, as study cases for this paper we present analyses concerning the behavior of the hottest fuel rod in a Pressurized Water Reactor during a shutdown wherein the residual heat removal system is lost (loss of the reactor's coolant pumps). These studies contemplate cases in which the fuel rod's geometry is ideal or curved. Analyses are also performed for two circumstances of positioning of the fuel inside the rod: concentric and eccentric.

1. INTRODUCTION

This study is part of an ongoing project at the Instituto de Engenharia Nuclear (IEN/CNEN) for thermo-hydraulic calculations on fuel rods of nuclear reactors. In the present work, we are concerned with the temperature behavior in fuel rods under unideal conditions, such as rods that have deformed cladding or dislocated fuel.

To analyze rods under the aforementioned conditions, a three-dimensional (3D) model is required. However, to keep the computational cost reasonable, it is sensible to avoid the use of the Navier-Stokes equations. Thus, we have chosen a physical model based on a 3D fuel rod coupled to a one-dimensional (1D) coolant channel.

Also aiming to study accidental conditions in which the coolant (light water) transcends its saturation temperature, turning into vapor, a homogeneous mixture is used to represent

Nomenclature

A	Area (m)	t	Time (s)	fo	of the outer surface of the fuel
a	Height (m)	T	Temperature (°C)	f	of saturated liquid
C_κ	Isobaric or Isochoric specific heat ($\mathrm{J\,kg^{-1}\,°C^{-1}}$)	V	Volume ($\mathrm{m^3}$)	fr	of the fuel rod
h	Specific enthalpy ($\mathrm{J\,kg^{-1}}$)	z	Direction z	g	of the gap
k	Thermal conductivity ($\mathrm{W\,m^{-1}\,°C^{-1}}$)	α	Void fraction	g	of saturated vapor
$\dot{m}$	Mass flow rate ($\mathrm{kg\,s^{-1}}$)	ρ	Density ($\mathrm{kg\,m^{-3}}$)	in	of the channel's inlet
p	Pressure (Pa)	Subscripts		m	of the homogeneous mixture
P	Perimeter (m)	0	of reference	max	maximum value
q'	Linear heat generation rate ($\mathrm{W\,m^{-1}}$)	c	of the cladding	med	mean value
q'''	Volumetric heat generation rate ($\mathrm{W\,m^{-3}}$)	ci	of the inner surface of the cladding	s	after shutdown
r	Radius (m)	cn	of the coolant channel	ss	of steady state
S	Surface	co	of the outer surface of the cladding	sat	of saturation
		f	of the fuel	w	of the outer surface of the fuel rod

the two-phase flow (liquid-vapor) of a single component, and so the coolant channel's energy equation is described using enthalpy.

Because our model uses temperature and enthalpy, the development of a fully coupled method for solving the pertinent equations became impractical. Therefore, the iterative method we called "internal iterations" was implemented, in which the conjugated heat transfer problem is solved in a segregated manner.

In the following sections we briefly describe the remaining attributes of the physical model adopted, the various correlations employed to estimate the thermal-hydraulic aspects of our problem, the methods used for the numerical discretization of the pertinent equations and the so called "internal iterations".

We also discuss about how the developed program was verified and present case studies in which the behavior of the hottest fuel rod in a Pressurized Water Reactor (PWR) is analyzed during a shutdown wherein the residual heat removal system is lost (loss of the reactor's coolant pumps). These studies contemplate cases in which the condition of the fuel rod's geometry is ideal or curved. Analysis are also performed for two circumstances of positioning of the fuel inside the rod: concentric and eccentric.

2. PHYSICAL MODEL

The three-dimensional transient heat conduction in the fuel rod is represented in this work by the variational formulation shown below:

$$\int_{V_{\mathrm{fr}}} \varphi\rho C_\kappa \frac{\partial T}{\partial t}\,\mathrm{d}V_{\mathrm{fr}} + \int_{V_{\mathrm{fr}}} k\vec{\nabla}T\cdot\vec{\nabla}\varphi\,\mathrm{d}V_{\mathrm{fr}} = \int_{V_{\mathrm{fr}}} \varphi q'''\,\mathrm{d}V_{\mathrm{fr}} - \int_{S_{\mathrm{fr}}} \varphi q''\mathrm{d}S_{\mathrm{fr}} \tag{1}$$

While, for the coolant channel's one-dimensional transient heat convection, it is employed the following differential form:

$$\rho A_{cn}\frac{\partial h}{\partial t}+\dot{m}\frac{\partial h}{\partial z}=\int\limits_{P_w} q''\,\mathrm{d}P_w \tag{2}$$

Equation (1) must be solved for each one of the components that constitute the fuel rod, which, essentially, are: fuel (UO_2), gap (filled with helium gas) and cladding (Zircalloy-4). The properties of these components, except for the densities ($\rho_f = 10\,963\,\mathrm{kg\,m^{-3}}$, $\rho_g = 0.1785\,\mathrm{kg\,m^{-3}}$ and $\rho_c = 6440\,\mathrm{kg\,m^{-3}}$), are considered in this paper to be temperature dependent. The same is true for the properties of the coolant, with the exception of the density in the two-phase regime, that is given by equation (3).

$$\rho_m = \alpha\rho_\mathrm{g} + (1-\alpha)\,\rho_\mathrm{f} \tag{3}$$

Regarding the components of the rod, we make use of the correlations recommended by the International Atomic Energy Agency (IAEA) [1] for the isobaric specific heat of UO_2 [1, p. 25]; and for the thermal conductivity of UO_2 [1, p. 89] and Zircaloy-4 [1, p. 249]. For the isobaric specific heat of Zircaloy-4 the correlation of Zimmerer [2] (as presented in [3, p. 1542]) is used. We also use correlations indicated by the IAEA [4] for the isochoric specific heat [4, p. 172] and the thermal conductivity [4, p. 173] of the helium gas.

Concerning the coolant, the routines of the code NBSNRCE [5] are used for most of its properties, the only exception being its enthalpy, which is provided by the IAPWS-IF97 [6], the Industrial Formulation 1997 from the International Association for the Properties of Water and Steam (IAPWS).

In this paper we consider the power of nuclear reactors under two circumstances: at nominal operation (steady state) and after the shutdown. The volumetric heat generation rate at steady state is given by equation (4):

$$q'''_f(z) = \frac{q'_{max_0}}{\pi r_f^2}\cos\left(\frac{\pi z}{a_\mathrm{fr}}\right) \tag{4}$$

As to the reactor's power after the shutdown, it essentially arises from fissions by delayed neutrons and the decay of fission products and actinides. Equation (5) [7, p. 65] is used o estimate the contribution of the former:

$$\dot{Q} = \dot{Q}_0\left[0.0625\exp(0.0124t_s) + 0.9375\exp(960t_s)\right] \tag{5}$$

The power derived from the decay of fission products and actinides is obtained from the fit presented in [8, p. 138] for the ANS standard (ANS FP + ^{239}U + ^{239}Np decay power curve).

The mass flow rate of the coolant is considered to be constant at normal operation whereas, in the shutdown, its behavior is dictated by equation (6), a fit for the data of Bordelon [9] relating to a typical pump of a Westinghouse's PWR.

$$\frac{\dot{m}}{\dot{m}_0} = \frac{1}{2}\exp\left[-4\left(\frac{t_s}{100^{0.91}}\right)^{0.85}\right] + \frac{1}{2}\exp(-0.06{t_s}^{0.73}) \tag{6}$$

As for the regimes of heat transfer contemplated in our studies, those of most importance are the single-phase forced convection and the flow boiling. The correlation of Dittus-Boelter/McAdams [10, 11] (as presented in [8, p. 567]) is used for the heat transfer in single-phase forced convection and the correlation of Chen [12] (as presented in [8, p. 752-755]) is adopted for the flow boiling heat transfer.

The critical heat flux, one of the most important phenomenon to be assessed, as its occurrence can irreversibly damage the fuel rod and even lead to its meltdown, was observed in our work to arise in the form of Dryout, which we assess with the correlation of Bowring [13] (as presented in [8, p. 781-782]).

The remaining simplifications adopted in our physical model, which are borne by equations (1) and (2), are: the fuel rod does not undergo thermal expansion; all the thermal energy generated by the rod is obtained in its fuel; there is no fluid motion in the gap and thus the heat transfer occurs in it only by conduction; no energy comes from reactions in the coolant channel; work due to the pressure gradient is small and can be ignored; the viscous-dissipation do not affect the thermal energy of the system; the axial conduction in the coolant can be disregarded; there is no mass or heat exchange between channels; and the cross-sectional area of the channel is constant.

2.1. Unideal Conditions

Besides a fuel rod with eccentric fuel, aiming to analyze the consequences of a possible irregularity in the manufacturing process of the fuel rod, we will also investigate the effects of an arbitrary curvature in the heat conduction of the rod.

Assuming a curvature in the x-direction over the entire fuel rod, represented by the longitudinal cut shown in Fig. 1, and approximating this deformation through circumference arcs, we obtained equation (7).

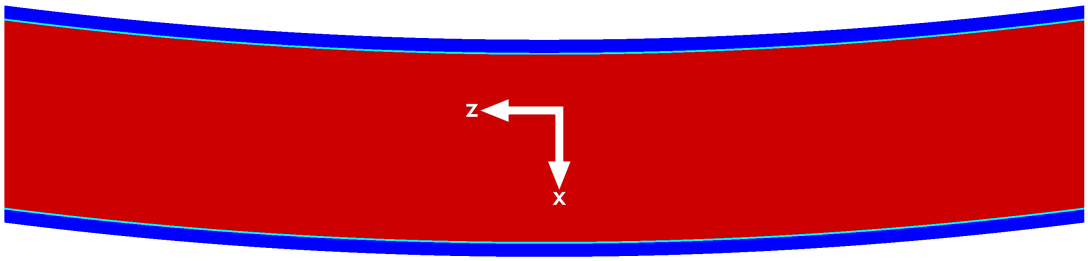

Figure 1: Curved fuel rod (longitudinal cut)

Note: Reduced rod, height equals to five times the diameter (1:77).

$$\delta_{cur} = \left[\left(\frac{a_{vc}^2 - 4\delta_{+max}^2}{8\delta_{+max}}\right)^2 - z^2 + z a_{vc}\right]^{1/2} - \frac{a_{vc}^2 - 4\delta_{+max}^2}{8\delta_{+max}} \tag{7}$$

where δ_{+max} is the maximum deformation $\left(\delta_{+max}\right)$, which occurs at half height of the rod.

In order to model the deformation, equation (7) is applied to the mesh of the rod with the use of: $x = x_a + \delta_{cur}$, where x_a is the former value of the x coordinate.

3. NUMERICAL MODEL

In our numerical model, we employ the finite element method for the spatial discretization of the dimensionless forms of equations (1) (fuel rod) and (2) (coolant channel). The Galerkin method, tetrahedral elements and linear base functions are adopted for the rod, whereas the least-squares method, linear elements and base functions are used for the channel. The discretization with respect to time, concerning both equations, is acquired through the Crank-Nicolson method.

Taking the average in each element for the physical properties of the rod's materials, the density of the coolant, the heat flux and the heat generation we reach the matrices for the fuel rod and the coolant channel. The matrix found for the rod is solved using the conjugate gradient method, in which the Jacobi preconditionner is applied [14]. Meanwhile, the matrix found for the channel is solved employing the Thomas algorithm.

4. INTERNAL ITERATIONS

The first step in the "internal iterations" is to evaluate the heat flux between the fuel rod and the coolant channel. Due to the rod possessing a three-dimensional discretization and the channel a one-dimensional, we use a structured grid as a mesh for the outer surface of the rod, produced by the means of the software GiD® [15], so to make sure that all nodes in any distinct height of the rod are connected to one node in the channel (Fig. 2), simplifying the calculation of the heat flux.

The most suitable experimental correlation (Dittus-Boelter/McAdams' or Chen's), according to the heat transfer regime contemplated at the instant analyzed, is used to obtain the heat flux. Its integral throughout the rod's perimeter is calculated by the means of the trapezium rule.

Since the equations are segregated due to the use of temperature for the rod and enthalpy for the coolant, the heat flux is calculated considering the thermal distribution of the previous time step (in reality the heat flux distribution achieved in the prior time step is employed, since it is already calculated considering the former thermal distribution).

Equations (1) and (2) are solved using the values found for the heat flux, then the distributions of temperature in the rod, enthalpy in the coolant and heat flux between

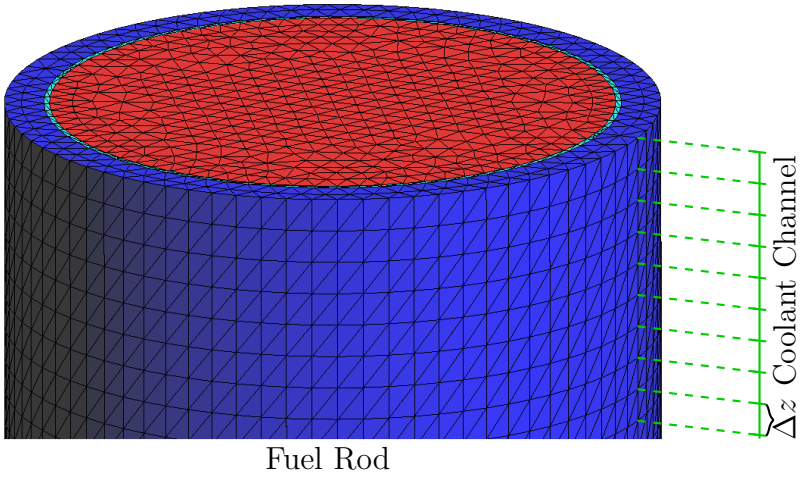

Figure 2: Discretization of the fuel rod and the coolant channel

them at the beginning and the end of this process are compared. If these distributions show a lower relative percentage difference than a pre-stipulated value, the code progresses to the next time step. Otherwise, the heat flux and the physical properties are recalculated using mean values for temperature and enthalpy, and the energy equations are solved again. The advance for the next time step only happens if enthalpy, temperature and heat flux reach equilibrium.

5. VERIFICATION AND VALIDATION

A series of tests were conducted in order to verify the developed program, among which were mesh convergence, convergence towards the steady state of simulations with different initial conditions of temperature and comparison of its results with those of an analytical solution for said state.

The iterative method adopted, "internal iterations", was verified by comparing results obtained through the developed program with those of a previous version of itself in which a fully coupled method was employed to solve the transient heat transfer restricted to the subcooled regime.

All the aforementioned tests provided great results, indicating no problems in the implementation of the program or the "internal iterations".

To verify and validate our findings in the flow boiling regime, we compared results provided by our code to those from the work of Krepper [16] and the experiment of Bartolomej [17] (as presented in [16, p. 723]).

The work of Krepper consists in the implementation of models for the subcooled boiling regime in the CFX® [18] software from ANSYS© with the purpose of investigating the capability of the computational fluid dynamics in contributing to the project of fuel assemblies, with emphasis in the improvement of heat flux and the prevention of critical heat flux.

As validation case Krepper made a simulation using data from an experiment of Bartolomej, which consists in an ascendant water flux through a heated tube with length of 2.0 m and diameter of $15.4 \cdot 10^{-3}$ m. In addition, the experiment had an uniform heat flux of $5.7 \cdot 10^5$ W m^{-2}, mass flow rate of 900.0 kg s^{-1} m^{-2} and $4.5 \cdot 10^6$ Pa of pressure. Krepper also adopted a two-dimensional cylindrical geometry and an input temperature 58.2 K below the saturation temperature of the coolant (light water), so that the equilibrium quality would be zero at 1.75 m of the tube's height.

To use the works of Krepper and Bartolomej for verification and validation, we adapted the parameters of the described problem into variables suitable for our code, that is, we modeled a coolant channel with the same hydraulic diameter as the heated tube of Bartolomej, and a fuel rod with a uniform heat generation rate that supplies the same heat flux.

We compared our findings for this problem with the data provided in [16] — extracted through digitalization, using the program Origin® [19] of OriginLab©, and converted to the Celsius scale — by the means of Fig. 3, which consists of a graph for the temperatures in the coolant, and in the surfaces of the fuel rod and the tube.

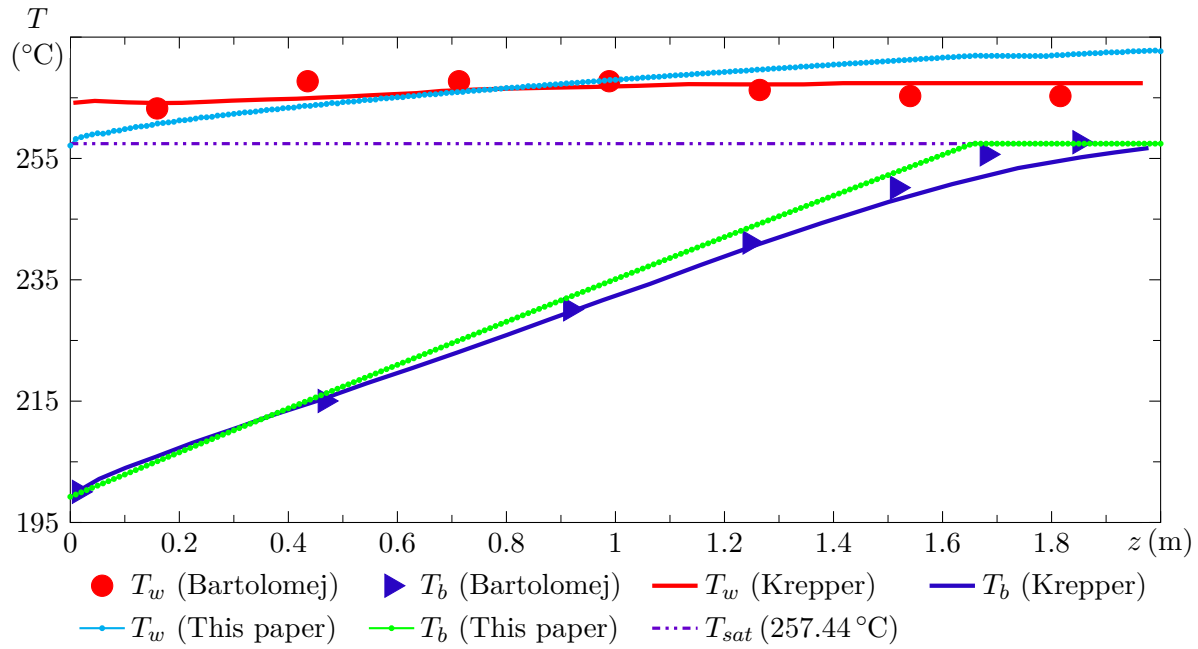

Figure 3: Temperatures of the validation case through the works of [16] and [17] (Data obtained from [16] with superimposed results)

As can be seen, our results for the temperature of the coolant are in agreement with the experimental data and the findings of Krepper. As for those concerning the temperature in the surface of the rod, they are underestimated at the beginning of boiling regime and overestimated at its end. Nonetheless the modeling applied in this work can reasonably represent the true behavior of the addressed phenomena, allowing us to satisfactorily conclude the verification and validation of the developed program.

6. CASE STUDIES

As case studies for this paper we analyze the shutdown transient of a PWR's hottest fuel rod in which the residual heat removal system is lost (loss of the reactor's coolant pumps), which means we concern ourselves with the heat transfer between the fuel rod and the coolant channel in the coastdown transient of the pumps. In these studies we contemplate not only a fuel rod with ideal conditions, that is, a rod with concentric fuel and perfect cladding (case called Ideal), but also rods with dislocated fuel (case Eccentric), and curved (case Curved).

The parameters of the reactor used in the studies are those from the Seabrook Station PWR, obtained form [8, p. 971-972] and presented in Table 1.

Table 1: Parameters of the Seabrook Station PWR (Data obtained from [8, p. 971-972])

Parameter	Value	Parameter	Value
p(Pa)	$15.51 \cdot 10^6$	p(m)	$12.6 \cdot 10^{-3}$
T_{in}(°C)	293.1	r_f(m)	$4.096 \cdot 10^{-3}$
$\dot{m}$(kg s^{-1})	0.335	r_{ci}(m)	$4.178 \cdot 10^{-3}$
q'_{max}(W m^{-1})	$44.62 \cdot 10^3$	r_{co}(m)	$4.75 \cdot 10^{-3}$
a_{fr}(m)	3.658		

As for the meshes used, we adopted one for rods with concentric fuel, and another for the rod with eccentric fuel, both produced by the means of the software GID and described by the parameters found in Table 2.

Table 2: Characteristics of the meshes used for the fuel rods studied

Parameter	Fuel Condition		Parameter	Fuel Condition	
	Concentric	Eccentric		Concentric	Eccentric
Divisions in the Height	100	100	Divisions in the Diameter	80	80
Elements	627 743	628 535	Nodes	110 576	110 761
in the Fuel	455 894	456 295	in the Fuel	81 464	81 551
in the Gap	49 235	48 661	in the Gap	16 372	16 283
in the Cladding	122 614	123 579	in the Cladding	28 900	29 087
in the Outer Surface	16 000	16 000	in the Outer Surface	8080	8080

The results will be presented through graphs relating to the spatial distribution and the temporal evolution of temperature in the fuel rod and the coolant channel, and enthalpy in

the channel. Special attention is given to four places in the rod: inner and outer surfaces of the cladding, outer surface of the fuel and center of the fuel. The results concerning surfaces are examined by the means of averages on their perimeters.

For rods with eccentric fuel, we consider six other places that are outlined in Fig. 4. These places comprehend positions in the direction in which the displacement occurs, and are further designated by the symbols d and e, that represent, respectively, the orientation favorable (right side) and opposite (left side) to the offset.

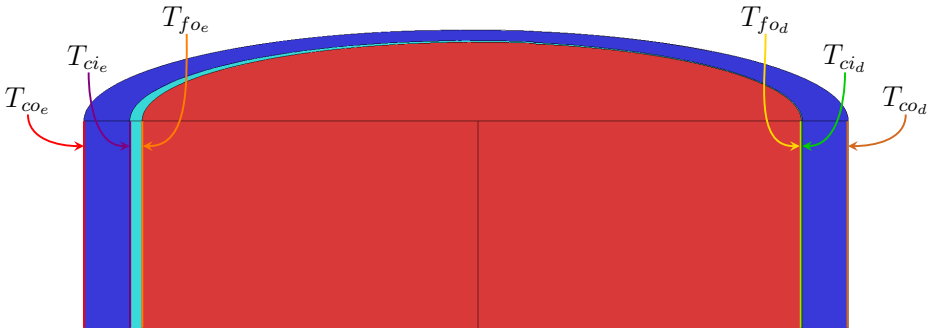

Figure 4: Representation of the additional locations of interest on an eccentric fuel rod

Finally, we point out that isolated the studies lose relevance, since it is due to the differences between them that their true value is revealed. For this reason, except for a few cases of interest, the results will be presented through comparisons with the case concerning the ideal fuel rod.

6.1. Fuel Rods with Concentric and Eccentric Fuel

An ideal fuel rod of the Seabrook Station PWR has a gap with thickness of $0.082 \cdot 10^{-3}$ m. For the case in which we analyze the heat transfer in a rod with eccentric fuel (case Eccentric), we designed the fuel of said rod with a displacement of $0.07 \cdot 10^{-3}$ m in the positive orientation of the x-axis, maximum value with which we were capable of generating a mesh using the adopted program for this purpose (GID). The fuel rod obtained, represented by Fig. 5, was called with eccentric fuel and in this section we will present the results achieved by its analysis compared to those of the ideal rod (case Ideal).

Fig. 6 shows the spatial distributions of temperature on the outer surface of the cladding (mean value) at the steady state of cases Ideal and Eccentric, as well as the spatial distributions of interest T_{co_d} and T_{co_e} referring only to the latter.

As we can see, the fuel's eccentricity causes the temperature distribution on the side of the cladding favorable to the offset to be a higher than the distribution on the opposite side. It is also apparent that the mean distributions of both cases overlap. The same manner is seen in the spatial temperature distributions on the inner surface of the cladding, with the difference between the distributions being only slightly more pronounced.

As for the temperature distributions on the outer surface of the fuel, the behavior reverses,

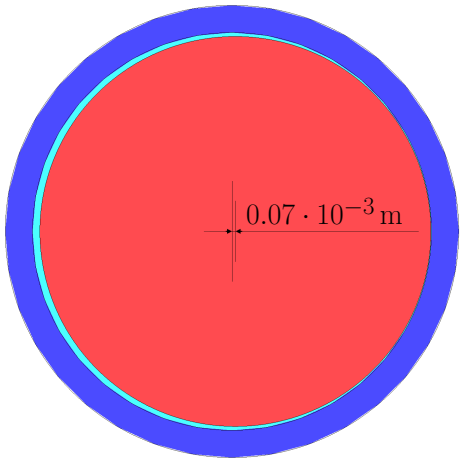

Figure 5: Rod with eccentric fuel

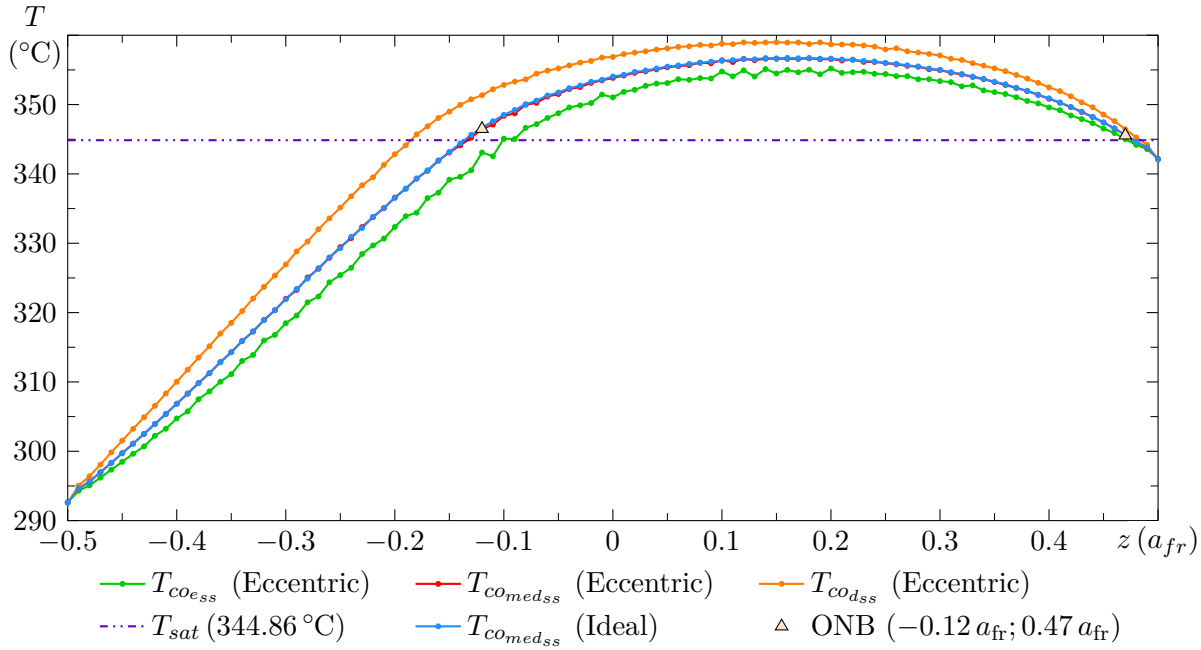

Figure 6: Spatial distribution of temperature in the outer surface of the cladding at steady state (cases Ideal and Eccentric)

with T_{fe_e} being greater than T_{fe_d}, Fig. 7, and its average in the perimeter being no longer equal to that of the ideal case.

We can attribute the aforementioned inversion, as well as the very existence of a difference between the distributions at the sides, to the fact that heat transfer between fuel and cladding is greater the smaller the gap thickness. This happens due to the filling of the gap by helium gas, as the gas sustains a much lower heat transfer than the UO_2 and Zircaloy-4, behaving in the form of a thermal resistance.

For a better appreciation of the temperature behavior in view of the fuel's displacement, we present the Figures 8 and 9, produced by means of the GID software, consisting of

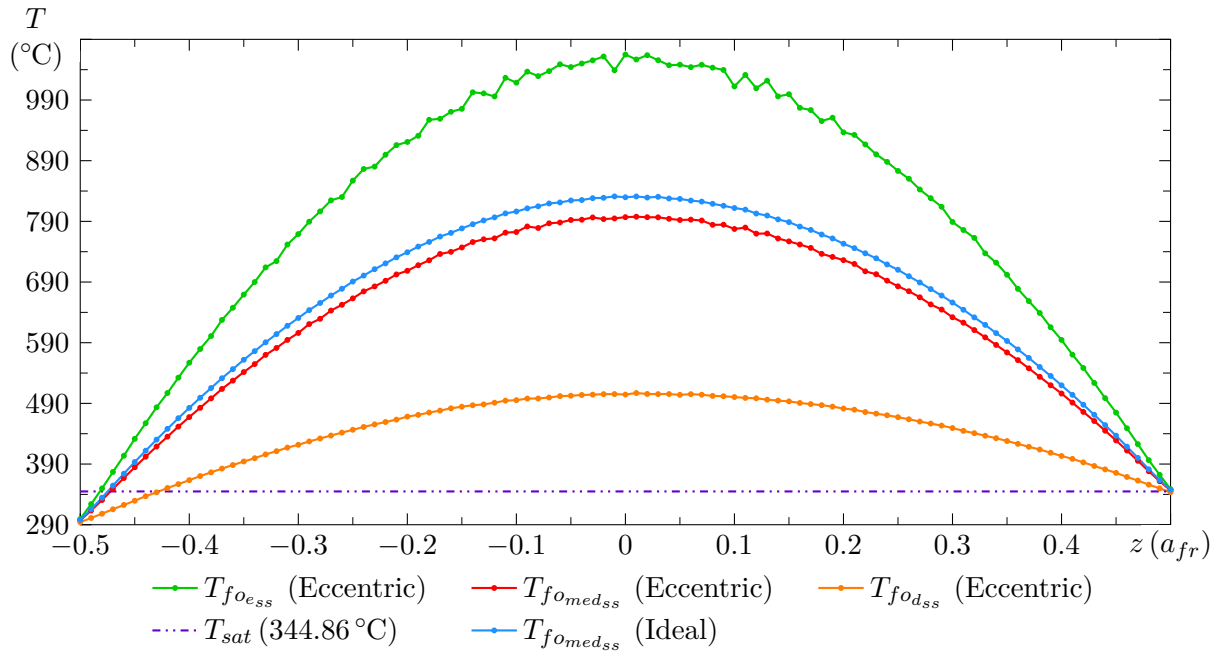

Figure 7: Spatial distribution of temperature in the outer surface of the fuel at steady state (cases Ideal and Eccentric)

transversal cuts[1] at half height of the spatial temperature distributions throughout the fuel rod, its cladding and its radius (only in the direction of displacement).

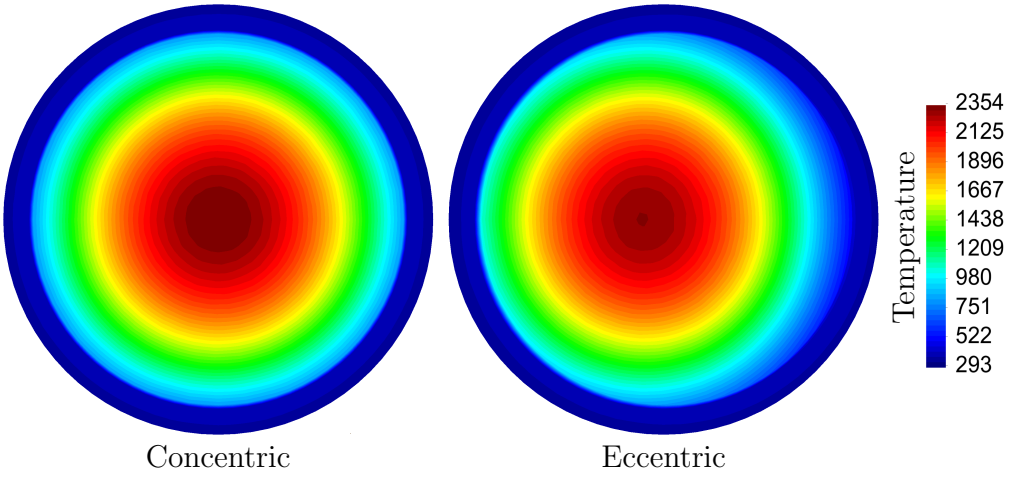

Figure 8: Transversal cuts of temperature distribution at steady state and half height (cases Ideal and Eccentric)

We can note from Figure 8 that, unlike the ideal case, the maximum temperature in the rod with eccentric fuel does not occur at its center line, nor does it coincide with the center line of the fuel, presenting a displacement from the middle of the rod proportional to the dislocation of the fuel, but in the opposite direction.

Completing the steady-state analysis, in Fig. 9, referring to the cladding of the cases

[1] we call transversal cuts of those that cross selected heights of the fuel rod in the radial direction

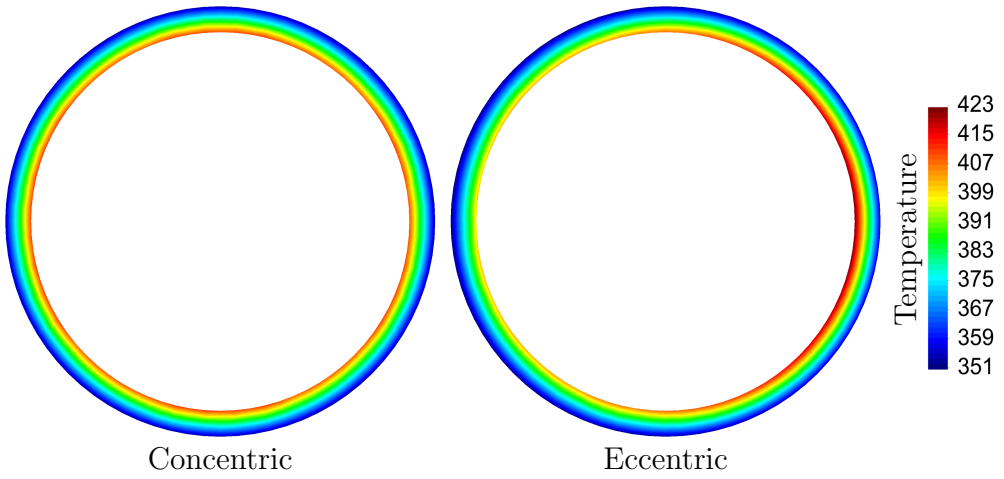

Figure 9: Transversal cuts of temperature distribution in the cladding at steady state and half height (cases Ideal and Eccentric)

investigated in this section, we observe how higher temperature levels occur in the lateral favorable to the fuel's displacement in the case Eccentric. Condition which, as mentioned, is associated with a more intense heat flow due to the greater proximity between cladding and fuel.

In regard to the coastdown transient of the pumps, in both simulations the Dryout phenomenon appears at the same height of the rod (0.43 a_{fr}) and at a very short time difference, respectively 365.52 s and 365.45 s, as shown by the temporal evolution of the coolant's enthalpy at the height in which the Dryout occurs, Fig. 10.

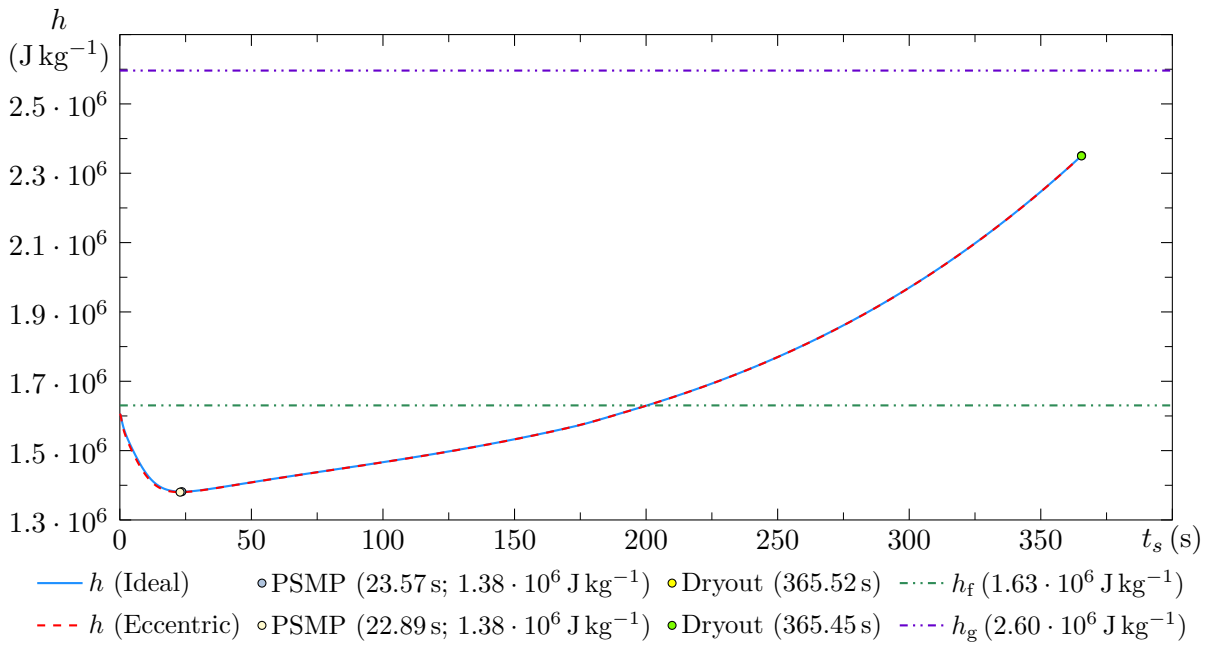

Figure 10: Temporal evolution of the coolant's enthalpy at the height in which the Dryout occurs (cases Ideal and Eccentric)

The characteristic of the temperature on the cladding's outer surface being different for

each side of the rod with eccentric fuel, with the side favorable to the fuel's dislocation showing higher temperature levels than those of the ideal case, led us to believe that a more intense heat flux would appear and, as consequence, the condition of critical heat flux would be anticipated. However, although there is difference between the temperatures and the fluxes on said sides, Figures 11 and 12, it barely affects the occurrence of Dryout.

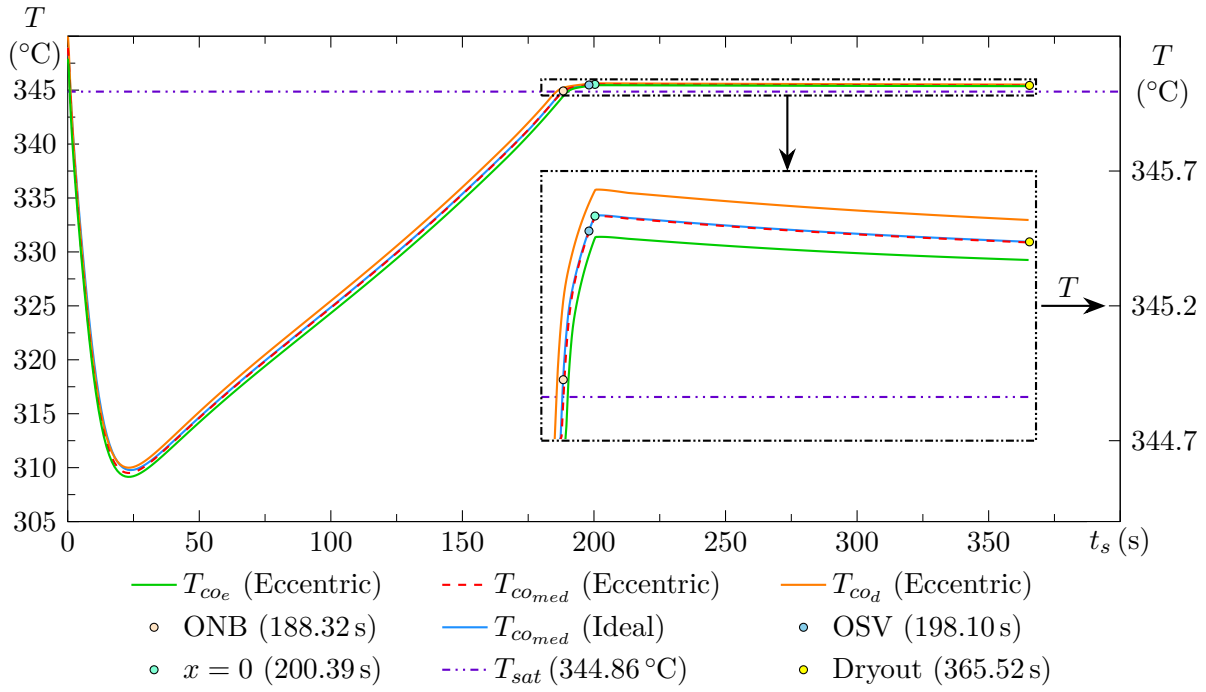

Figure 11: Temporal evolution of the cladding's outer surface temperature at the height in which the Dryout occurs (cases Ideal and Eccentric)

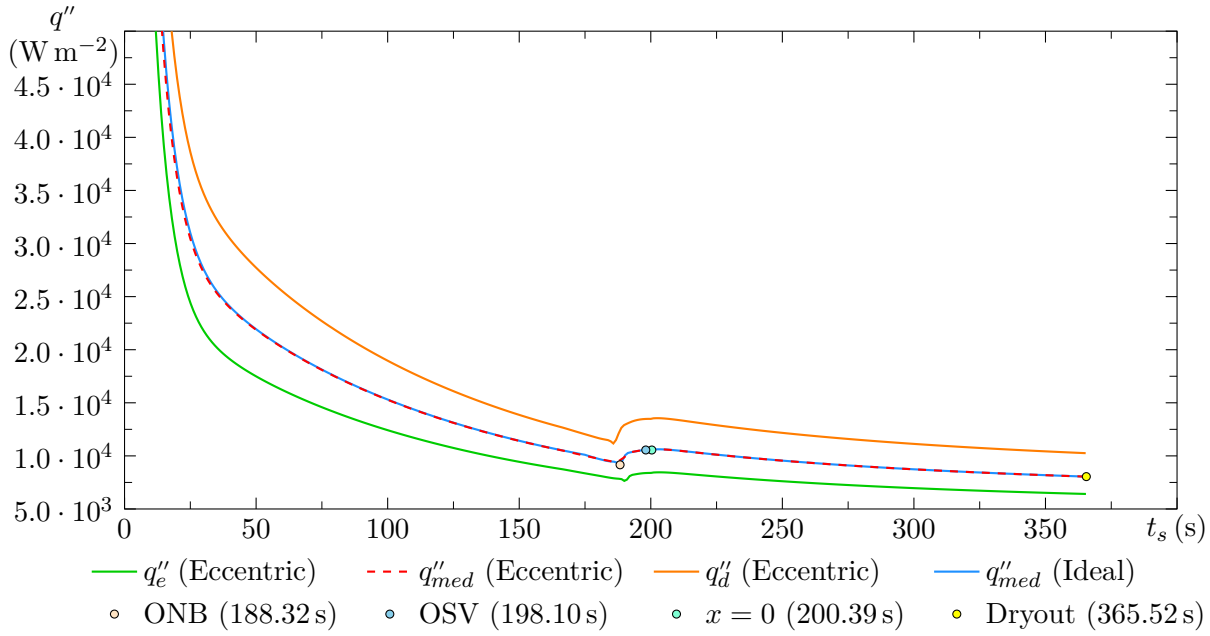

Figure 12: Temporal evolution of heat flux between rod and channel at the height in which the Dryout occurs (cases Ideal and Eccentric)

Knowing that the Dryout has a strong dependence on the flow quality, which increases rapidly shortly before the Dryout appears, and is maximum at the height where it happens. We can reason that the similarity between both cases in regard to the conjunctures in which the Dryout occurs derives from the lack of spatial variation in flow quality throughout the perimeter of the rod, due to the one-dimensional model of the channel.

Also shown in Fig. 10 is the post-shutdown minimum point (PSMP), that represents the moment, at the analyzed height, in which the removal of heat by the inertia of the pumps is no longer sufficient to cool the channel, that is, at this instant the "production" of heat in the fuel rod and the removal by the coolant channel equalize in the height in question and henceforward the temperatures tend to increase.

In Figures 11 and 12, we can also see the transition points between the regimes of heat transfer discussed in section (2.) and, as consequence, relate the improvement of heat flow to the PSB regime as well as the stability of temperature on the outer surface of the cladding to the SNB regime.

Finally, in order to complete this case study, we provide Figures 13a and 13b, which serve as a representation for the temporal evolution of temperature in the rod with eccentric fuel generated by means of longitudinal and transversal cuts in said rod at selected instants. It is important to note that the height of the rod is reduced in the longitudinal cuts, so the temperature distribution in them should be contemplated considering the deformation in the direction affected.

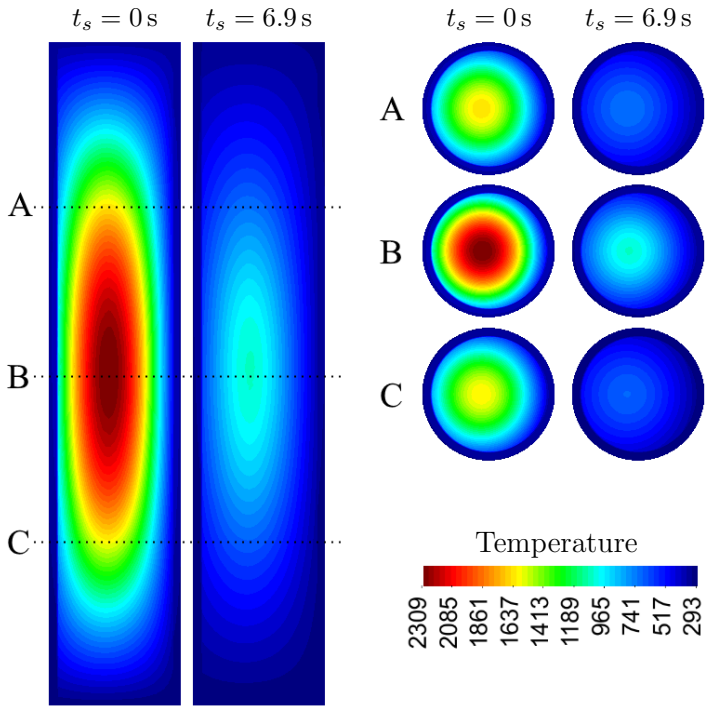

Figure 13a: Longitudinal and transversal cuts of temperature distribution in the rod with eccentric fuel at selected instants

Note: Reduced rod, height equals to five times the diameter (1:77).

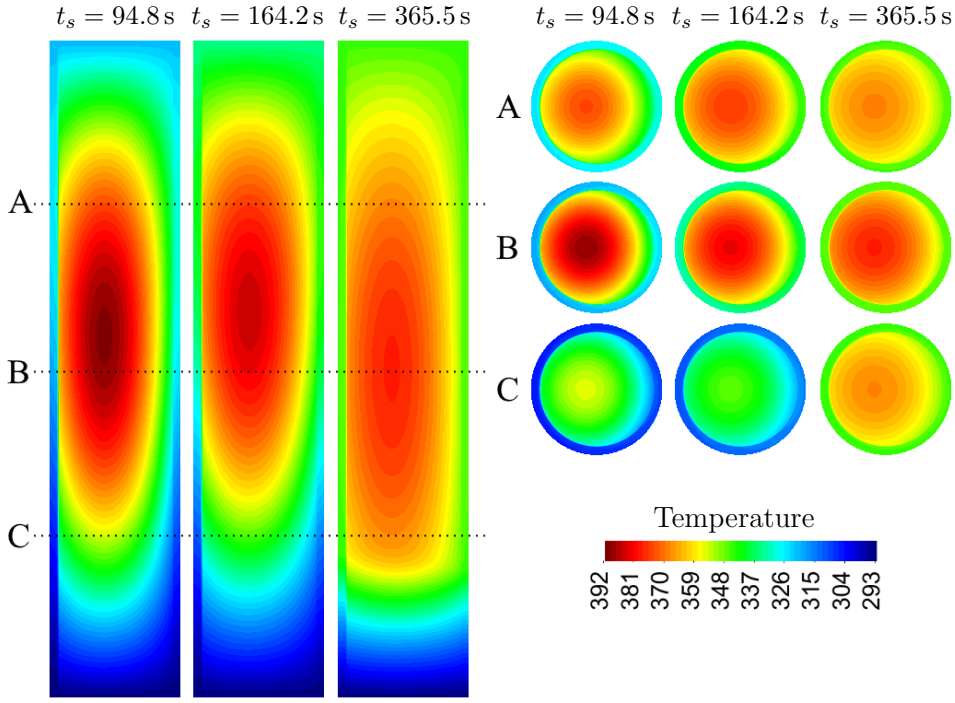

Figure 13b: Longitudinal and transversal cuts of temperature distribution in the rod with eccentric fuel at selected instants

Note: Reduced rod, height equals to five times the diameter (1:77).

Through Figures 13a and 13b we can see that the displacement in the temperature distributions shown in the steady state propagates throughout the simulation. We also notice how the temperature in the fuel rod decreases rapidly after the shutdown of the reactor begins, even though its pumps are also turned off. Subsequently we observe how the temperature begin to rise in the upper part of the rod, process that spreads to the lower part until the moment in which the Dryout condition is reached, finishing our simulation.

6.2. Ideal and Curved Rods with Concentric Fuels

The spacing between the outer surface of the rod and the extremity of the coolant channel is of $1.55 \cdot 10^{-3}\,\mathrm{m}$, Fig. 14. For the study corresponding to this section we modeled a fuel rod with concentric fuel and maximum deformation ($\delta_{+_{max}}$) of approximately one-third of the referred space, $0.5 \cdot 10^{-3}\,\mathrm{m}$ (case Curved), and compared the achieved results with those from the ideal fuel rod (case Ideal).

By the means of the obtained data, we verified that the applied curvature exerts an inexpressive influence on the temperature distribution of the fuel rod, assertion corroborated not only by the fact that cases Ideal and Curved presented the same conditions of Dryout (365.52 s, 0.43 a_{vc}), but especially for the low percentage difference between the temperatures of both cases, less than $4.0 \cdot 10^{-2}\,\%$. Evaluation performed considering each of the 110 761 nodes that constitute the mesh used (in both cases the same mesh is used, the difference being the deformation applied for the curved case using equation (7)), and three instants: when the steady state is reached, when the Dryout occurs, and just about

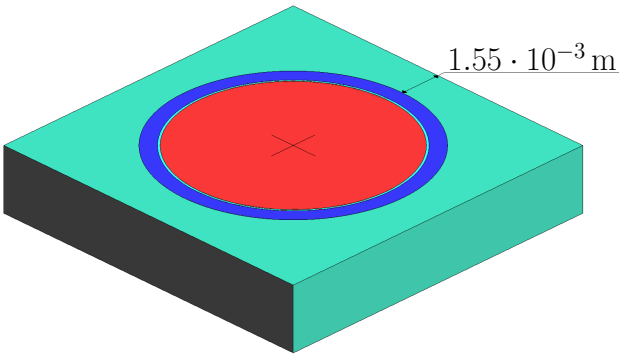

Figure 14: Representation of a fuel rod with its coolant channel

half the time interval between said moments.

The only difference between the Ideal and the Curved cases, as shown by the longitudinal cuts shown in Fig. 15[2], is the curvature itself.

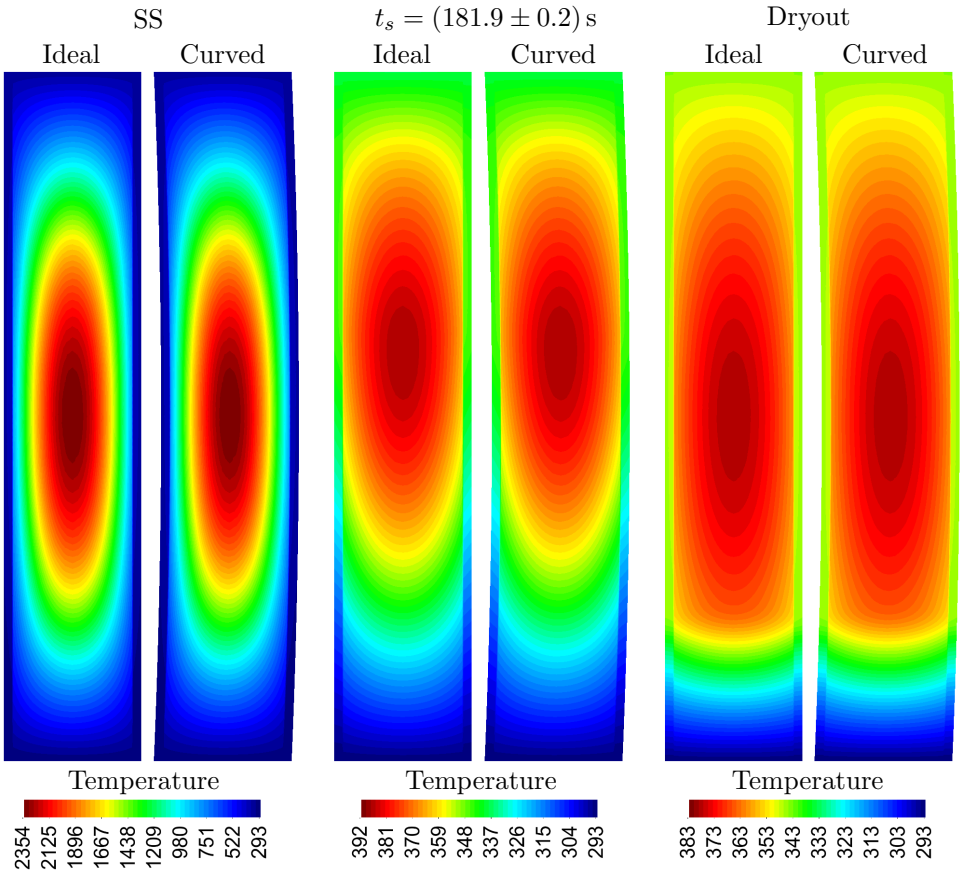

Figure 15: Longitudinal cuts of temperature distribution in the rods of the cases Ideal and Curved at selected instants

Note: Reduced rod, height equals to five times the diameter (1:77).

[2]the uncertainty of 0.2 s seen in this image derives from fact that, with the exception of the moments in which the steady state is reached and Dryout occurs, we cannot compare the exact same time instant of both cases, due to how the temperature data of the entire mesh is recorded

Although the curvature applied to the rod is very small in comparison to its height, it is reasonable to assume that the conformity exhibited by the analyzed cases is mainly related to the limitations imputed to the code by the 1D modeling of the coolant channel, since it renders the reproduction of radial asymmetries in the channel unfeasible.

7. CONCLUSIONS

In this study we saw how the eccentricity of a fuel rod's fuel causes higher temperatures to emerge on the side of the cladding to which the fuel dislocates. A condition that inverses in the fuel, with the increase of temperature happening in the opposite direction of the displacement.

No significant effect was observed on the fuel rod temperature distribution due to the curvature analyzed, with the percentage difference in temperature, compared to the results from the ideal rod, being less than $4.0 \cdot 10^{-2}$ %.

We conclude that the temperature variation in the case with eccentric fuel occurs due to the gap presenting itself as a "resistance" to the heat transfer between fuel and cladding. We also assume that the lack of change in the case of the curved rod, compared to the ideal case, can be associated with the 1D model of the coolant channel.

Regarding the shutdown transient, in which the residual heat removal system is lost (loss of the reactor's coolant pumps), all simulations presented the phenomenon of Dryout at the same height of the fuel rod and at similar instants of time. We conclude that this similarity is essentially associated with the high dependence of the CHF on the flow quality, and with the fact that, due to our 1D modeling, the flow quality distribution is identical in all cases.

In the reactor's shutdown we contemplated the temperature behavior in the studied fuel rods, from its rapid decrease at the beginning of the transient, through its increase in the upper parts of the rods, which propagates to the lower parts, until the condition of Dryout occurs. We also observed the reproduction, at all steps of the simulations, of the effects caused by the eccentricity of the fuel.

Finally, we condescend with the fact that the physical simplifications we adopted to describe the phenomenon discussed, the heat transfer in fuel rods, have caused restrictions to our studies, mainly the 1D modeling of the coolant channel. Nevertheless, this work has gathered opportune results, revealing circumstances of interest on the problem investigated, thus contributing to its knowledge.

REFERENCES

1. IAEA, "Thermophysical Properties Database of Materials for Light Water Reactors and Heavy Water Reactors", *International Atomic Energy Agency*, Vienna (2006).
2. W. Zimmerer, "Darstellung der neu Integrierten Stoffdaten-funktionen im System Maplib in Tabellarischer und Graphischer Form", *Kernforschungszentrum Karlsruhe*, Tech. Rep. KfK-Ext.8/78-3, (1978).

3. D. G. Cacuci, *Handbook of Nuclear Engineering: Vol. 1: Nuclear Engineering Fundamentals; Vol. 2: Reactor Design; Vol. 3: Reactor Analysis; Vol. 4: Reactors of Generations III and IV; Vol. 5: Fuel Cycles, Decommissioning, Waste Disposal and Safeguards*, Springer Science & Business Media, (2010).
4. IAEA, "Thermophysical Properties of Materials for Water Cooled Reactors", *International Atomic Energy Agency*, Vienna, (1997).
5. M. D. L. Moreira, D. A. Botelho, "Subrotina de Propriedades Termodinâmicas da Água", *CNEN/IEN*, Rio de Janeiro (1992).
6. J. R. Cooper, R. B. Dooley, "Revised Release on the IAPWS Industrial Formulation 1997 for the Thermodynamic Properties of Water and Steam", *The International Association for the Properties of Water and Steam*, Lucerne, Switzerland, August (2007).
7. N. E. Todreas, M. S. Kazimi, *Nuclear Systems 1*, Taylor & Francis Goup, (1990).
8. N. E. Todreas, M. S. Kazimi, *Nuclear Systems: Thermal Hydraulic Fundamentals*, CRC Press, (2011).
9. F. M. Bordelon, "Calculation of Flow Coastdown After Loss of Reactor Coolant Pump (Phoenix Code)", *WCAP - 7973*, (1972).
10. F. W. Dittus, L. M. K. Boelter, "Heat Transfer in Automobile Radiators of the Tubular Type", *University of California, Berkeley. Publications in English*, **2**, pp. 443–461, (1930).
11. W. H. McAdams, *Heat Transmission*, McGraw-Hill, New York, USA (1942).
12. J. C. Chen, "Correlation for Boiling Heat Transfer to Saturated Fluids in Convective Flow", *Industrial & Engineering Chemistry Process Design and Development*, **5**(3), pp. 322–329, (1966).
13. R. W. Bowring, "A New Mixed Flow Cluster Dryout Correlation for Pressures in the Range 0.6–15.5 MN/m^2 for Use in a Transient Blowdown Code", *Proceedings of the IME Meeting on Reactor Safety, Paper C217*, Manchester (1977).
14. P. A. B. De Sampaio, "Heat_Transfer_2d_cg.f90", CNEN/IEN, Rio de Janeiro (2007).
15. A. Melendo, A. Coll, M. Pasenau, E. Escolano, A. Monros, "GiD®", `http://www.gidhome.com`, Access date: 29 Jun. (2016).
16. E. Krepper, B. Končar, Y. Egorov, "CFD Modelling of Subcooled Boiling—concept, Validation and Application to Fuel Assembly Design", *Nuclear Engineering and Design*, **237**(7), pp. 716–731, (2007).
17. G. G. Bartolomej, V. M. Chanturiya, "Experimental Study of True Void Fraction When Boiling Subcooled Water in Vertical Tubes", *Thermal Engineering*, **14**(7), pp. 123–128, (1967).
18. ANSYS, "ANSYS-CFX®", `http://www.ansys.com/Products/Fluids/ANSYS-CFX`, Access date: 27 ago. (2016).
19. OriginLab, "Origin®", `http://www.originlab.com`, Access date: 29 Jun. (2016).